Dry friction experiments: Slider in a turntable

Author: Albert Abio Rojo
Facultat de Física, Universitat de Barcelona, Diagonal 645, 08028 Barcelona, Spain.

Advisors: Jordi Ortín and Ramon Planet

Abstract: Friction theories have been developed for centuries. Even so, most of them are empirical and there are many cases where the experimental results cannot be explained with the models. The principal cause of this fact is the nonlinearity of friction problems. The aim of this work is to study dry friction with the design of an experimental setup based in a slider on a turntable attached into an external fixed point. The implementation of a tracking program is needed to follow the slider trajectory. In particular, stick-slip phenomena has been produced with mass-spring system with two degrees of freedom. We have done a qualititative analysis of the results comparing them with the steady sliding case, in order to understand better the nonlinearity of friction. In addition, we have solved numerically the equations of motion of the slider in the framework of Coulomb model of friction to compare the solution with the experimental results. Our study shows that friction is a non-linear problem and that Coulomb model is not valid to explain our experiment but can predict the period of stick-slip oscillations.

I. INTRODUCTION

Friction is understood as the resistive force between contact surfaces that opposes their relative motion. Despite being an important problem in science due to its relevance in engineering, industrial processes, geophysics and solid mechanics in general, there is no established model to explain the mechanism of macroscopic friction. In fact, there are no fundamental equations in friction, only empirical models that try to explain the experimental results.

However, some ideas about macroscopic friction are widely accepted, such as the differentiation between two types of friction: static and dynamic friction. Static friction is considered a resistive force that opposes any applied force to a body resting on a surface; it keeps the body at rest. On the other hand, dynamic friction is the contact force against the motion relative to a surface on which it slides. Both types of friction are governed by static and dynamic coefficients, μ_s and μ_d, respectively. Those ideas provide nonlinearity to friction.

In this work we will focus in the problem between two solids that are directly in contact, i.e. without an intermediate fluid lubrication layer. In this context, many models try to describe dry friction. The most known model is the Coulomb model [1], which is a totally empirical model based in the classical Amontons-Coulomb laws of friction [2]: i) Both μ_s and μ_d do not depend on the normal force or the area of the contact. ii) μ_s and μ_d depend only on the materials in contact. iii) In general, $\mu_s > \mu_d$.

Coulomb model is governed by the following equations:

$$F_C = \mu F_L, \tag{1}$$

where F_C is the Coulomb force, F_L is the load (force in the normal to the contact surface) and μ can be either the static (μ_s) or dynamic (μ_d) frictional coefficient (this differentiation between the frictional coefficients is a modification from the original Coulomb model). When the difference between static and dynamic friction is taken into account, the friction force (F_f) in the body (slider) in this model is written as:

$$F_f = \begin{cases} F_C \cdot sign(\dot{x}) & \text{if} \quad \dot{x} \neq 0, \\ F_{app} & \text{if} \quad \dot{x} = 0, F_{app} < F_C, \end{cases} \tag{2}$$

where $\dot{x}$ is the relative velocity between the slider and the surface, $sign$ is the sign function and F_{app} is the external force applied to the slider.

Coulomb model is broadly used to describe dry friction, due to its simplicity. However, there are more complex models that capture dry friction with more accuracy. For example, Stribeck model is relevant because it considers lubrication between surfaces that causes a dependence of the friction force and the sliding speed; and Dahl model assumes that friction force is only dependent on the displacement and it has important applications in control engineering [1].

Another mechanism to understand friction is the adhesion theory introduced by Bowden and Tabor [3, 4]. This theory is based on the roughness of the surfaces in contact at the μm scale, that implies that the real contact area is different from the apparent contact area because the surfaces touch each other only in some contact points called asperities. The models derived from the adhesion predict a time dependence in the static friction coefficient, and velocity and contact memory dependence in the dynamical friction coefficient. This has been proved experimentally [2, 5–7]. The highly nonlinear behavior of friction is the main cause of complexity in friction problems and it provoques serious difficulties in predicting some non-intuitive events that occur in friction dynamics.

One of the phenomena expected in dry friction is stick-slip motion. Stick-slip motion is defined as the temporal succession of static (stick) and dynamic (slip) states. The difference between the values of static and dynamic friction coefficient, i.e. static and dynamic friction force, is a reason of the manifestation of stick-slip. Another cause of stick-slip is the velocity dependence of the friction coefficient. In the framework of the adhesion theory, this type of movement occurs when the asperities between the surfaces cannot longer hold the shear stress (stick) and break (slip) into new asperities that must be rearranged for the system [8]. There are many system that present stick-slip behavior, for example earthquakes [2, 8] in geophysics or brake pads and wind turbines in engineering, where it is a harmful problem. Despite its importance, there is no general stick-slip accepted model and each specific problem uses its particular friction model. [5].

In this work, we have designed and performed an experiment of dry friction where an slider attached to an inextensible thread or a spring is moving on a rotating disk. The mass-spring system is a usual way to model stick-slip [6]. We expect that the nonlinear character of friction will give rise to stick-slip motion. We will compare our experimental data with a numerically-simulated dynamic behavior of Coulomb model.

II. MATERIALS AND METHODS

A. Experimental setup

The experimental setup consists in a circular turntable with radius of 20 cm and a solid body on the turntable attached into a fixed point (P) at a distance of 24.0 ± 0.2 cm to the center of the turntable, using either a thread or a spring (Fig.1a). The turntable rotates around its axis in counter-clock wise direction. A motor with a control box produces the rotation. In this work only three angular velocities are used: $\Omega_1 = 4.68 \pm 0.12$ rpm, $\Omega_2 = 14.61 \pm 0.09$ rpm and $\Omega_3 = 25.05 \pm 0.06$ rpm. Then, the solid body will slide on the surface of the table, which has been covered with a soft plastic layer. The slider used in all the acquisitions is a disk of stainless steel (dimensions shown in Fig.1b) with a lug situated in the lateral of the disk and a vertical bar situated on the mass center. The mass of the disk can be modified adding disks of steel with a central hole that passes through the vertical bar. The masses used are $M_1 = 102.509 \pm 0.001$ g, $M_2 = 152.509 \pm 0.001$ g and $M_3 = 202.509 \pm 0.001$ g.

The thread is a nylon of lenght $a = 19.0 \pm 0.2$ cm. It is considered inextensible and its mass is neglected. The spring has an elastic coefficient of $k = 4.84$ N/m and its natural length is $L_0 = 19.0 \pm 0.2$ cm. Its mass must be taken into account in the discussion of the results. The lug in the slider allows to link it to the fixed point P using either the thread or the spring. The lenght of $a \simeq 19$ cm has not been chosen arbitrarily. This value is needed to keep the slider on the surface of the turntable and to eliminate its own rotation.

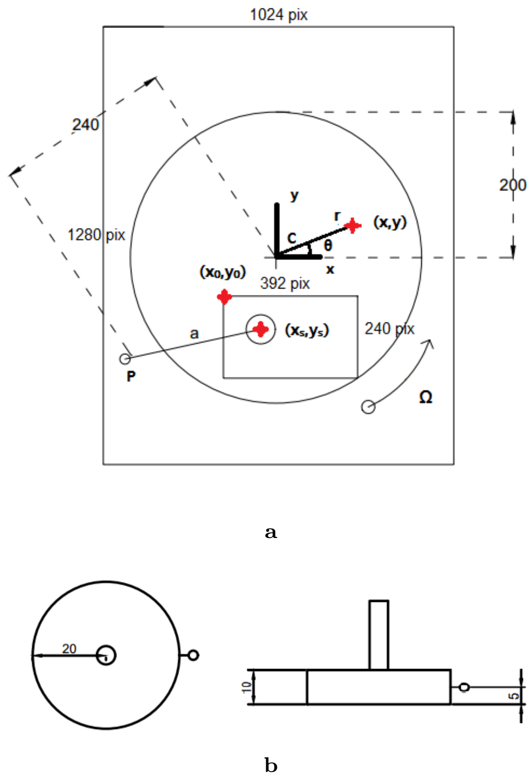

FIG. 1: a) Snapshot of the turntable setup from above and the region caught by the camera with the chosen ROI, with the pixels of each region indicated. The values of the distances are in mm. The lenght a depends on the experiment. b) Snapshot of the slider from an axial and a lateral point of view. The values are in mm.

The data of the center of mass of the slider will be obtained by a filmation of the experiment from above. For this reason, the turntable is inside a chamber made of black porexpan walls. To have homogeneous lightning, four fluorescent lights are placed facing the top porexpan surface of the chambers. A videocamera (Motion Pro X3) is situated on the top in order to film the experiments through a hole in the top wall.

An important part of our work has been the design of the experimental setup and the tracking software described in the next section. The analysis of the results are original as well. Although we find out that the setup is very similar to the one proposed by Tapia, Le Tourneau and Géminard [9], the design and the results are new and original. The data obtained from the experiments will be the positions of the center of mass of the slider on the turntable.

B. Data acquisition and processing

The videocamera has a resolution of 1280×1024 pixels, which corresponds to a spatial resolution of $0.047 \pm$

0.001 cm/pixel. With the acquisition software of the videocamera (Motion Studio), a ROI of 392 × 240 pixels and height 240 pixels has been chosen and centered in the region where the slider moves in each acquisition. The frequency will be 100 frames/s (i.e $\delta t = 0,01$ s between consecutive images), to avoid the 50 Hz flickering of the light intensity. The mentioned parameters have been determined after several trials of acquisitions.

The images are obtained in grayscale, and they are processed with an original Python tracking program based in the OpenCV library. The program use a contrast filter to select the slider over all the image. After this selection, a Gaussian smoothing is applied to reduce the noise. Then, the program detects the slider boundaries allowing to compute the image moments (weighted average of the intensity of the image pixels) and its centroid. If we assume that the density of the slider is constant, the centroid corresponds to its center of mass. Figure 2 shows the steps of the image processing.

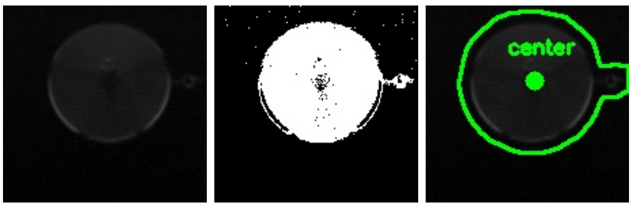

a **b** **c**

FIG. 2: Steps of the tracking program: a) Grayscale image from the videocamera. b) Selection of the slider over all the image. c) Detection of the boundaries and the center of mass.

The final outputs of the program are the positions of center of mass of the slider as a function of time. These positions are relative to the (x_0, y_0) of the ROI. The positions can be expressed in a reference system centered in the center of the turntable. It is possible to express the positions either in cartesian coordinates or in polar coordinates (Fig. 1a). Using the spatial resolution, the pixels are changed into cm. There are two possible frames to work: the laboratory frame O or the frame of the turntable O':

$$\begin{cases} (x, y) \to (x' = R\cos(\Omega t), y' = R\sin(\Omega t)) \\ (r, \theta) \to (r' = r, \theta' = \theta + \Omega t) \end{cases} \tag{3}$$

where (x, y) and (x', y') are the cartesian coordinates, (r, θ) and (r', θ') are the polar coordinates, Ω is the angular velocity of the turntable and t is the elapsed time.

The angular velocity of the turntable is determined using the tracking program as well. A fixed piece of white paper is put on the turntable and it is detected by the program as it moves with the turntable.

III. RESULTS AND DISCUSSION

In this section, the case of the slider attached to the nylon thread is taken as a reference, in order to compare it with the spring-mass system.

The figures obtained do not include error bars because they will not be relevant and the discussion of the results will be qualitative. Smoothing with splines has been applied in some figures, but it does not eliminate any relevant behavior. The derivative of the radius and the angle has been done using this smoothing technique to fit a function and compute its numerical derivative.

From Coulomb model (Eqs. (1) and (2)), the equations of motion of the slider can be written as [10]:

$$\begin{cases} (\ddot{r} - r\dot{\theta}^2)\hat{r} = \left(\frac{-\mu g \dot{r}}{\sqrt{r^2(\Omega-\dot{\theta})^2+\dot{r}^2}} + \frac{F_r}{M} \right)\hat{r} \\ (2\dot{r}\dot{\theta} + r\ddot{\theta})\hat{\theta} = \left(\frac{\mu g r(\Omega-\dot{\theta})}{\sqrt{r^2(\Omega-\dot{\theta})^2+\dot{r}^2}} + \frac{F_\theta}{M} \right)\hat{\theta} \end{cases} \tag{4}$$

where r and θ are the polar coordinates, $g = 9,81$ m/s^2, Ω is the angular velocity of the turntable and F_r and F_θ are the radial and azimuthal components of the applied force (elastic or tensile) components.

A. Effect of M and Ω

The first step is to determine the effect that some parameters have on the sliding. Therefore, the dependences of r and θ with time for different masses and angular velocities is studied (Figs. 3 and 5).

As anticipated [9], the nylon thread case is almost a steady sliding case, since the radius and the angle do not show relevant changes in time (Figs. 3a, 3c, 4a and 4c). Neverthless, some interesting ideas can be extracted: i) r decreases with the increment of mass. ii) θ also decreases wih the increment of mass. iii) The small oscillations of r (in θ they are not detected) have a periodicity corresponding to the turntable rotation. Since the surface is not perfectly flat, this can be associated to small surface roughness that the slider encounters during its motion. The effect is that the sliding is not perfectly steady, due to a change in the friction coefficient in points where the surface has irregularities. It shows how sensible friction is to the contact of the surfaces, as the adhesion theory predicts [3, 4].

In the spring case (Figs. 3b, 3d, 4b and 4d), statements i) and ii) become more evident due to the change into a elastic applied force. Another reason is that the mass of the spring is greater than the nylon mass. There are some remarkable facts: iv) The amplitude of large oscillations in radial direction is enhanced for large masses and for low angular velocities. If the mass is small and the angular velocity is large, the behavior is similar to the one with the nylon link, i.e. oscillations practically disappear. v) The angle decreases and the amplitudes of

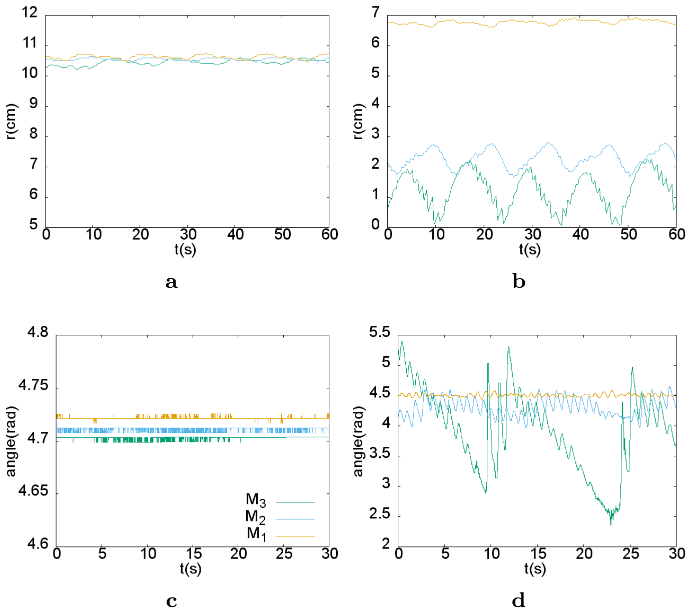

FIG. 3: r and θ as a function of time for different mass in the laboratory frame (O). $\Omega = \Omega_1$. A smooth vith splines has been applied. (a) $r(t)$ with nylon thread. (b) $r(t)$ with spring. (c) $\theta(t)$ with nylon thread. (d) $\theta(t)$ with spring.

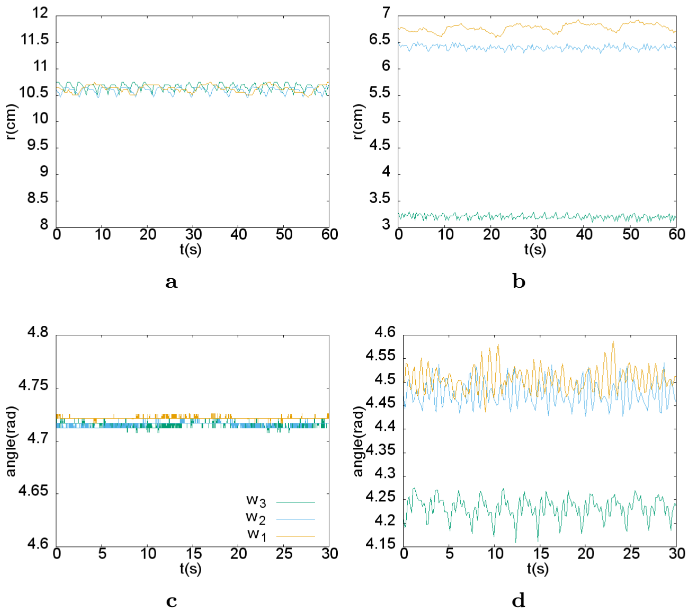

FIG. 4: r and θ as a function of time for different angular velocities in the laboratory frame (O). $M = M_1$. A smooth with splines has been applied. (a) $r(t)$ with nylon thread. (b) $r(t)$ with spring. (c) $\theta(t)$ with nylon thread. (d) $\theta(t)$ with spring.

oscillations become more regular with the increase of the angular velocity. The obtained results seem to confirm the dependences of stick-slip on both the mass and the driving velocities found in previous works [6, 7].

Two types of oscillations can be observed: 1) The harmonic behaviour of the mass-spring system produces a stick-slip of low amplitude and high frequency. 2) A change of the relative velocity between the turntable and the slider produces a large amplitude stick-slip of the frequency of the turntable rotation. This occurs when the slider approaches the center of the turntable, and even passes from the bottom(top) to the top(bottom) half of the turntable for the largest mass. This change affects drastically in the system dynamics and can be explained with a stick phase (when the slider is approaching to the center) and a slip phase (the slider moves rapidly away from the center). The slip phase hides the low amplitude oscillations.

These preliminary results and observations allow to fix the values of the mass and the angular velocity in order to extend the study for a particular case where stick-slip is more relevant. The selected values are $M = M_3$ and $\Omega = \Omega_1$.

It is interesting to represent the slider trajectory in the turntable reference frame (O') when the body is attached to the spring, and in the particular case $M = M_3$ and $\Omega = \Omega_1$. For the nylon thread, the trajectory is a circle in O' and it is not a relevant case to study. In Fig. 5a,

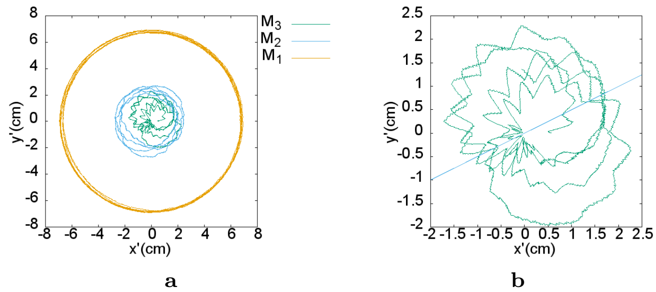

FIG. 5: Trajectory of the slider the turntable reference frame (O'). In different cases. Link: spring. (a) $\Omega = \Omega_1$ and different masses. (b) Particular case. M_3 and Ω_1. The blue line separates two regions.

the effect of the mass mentioned before is evident in the trajectory of the slider. In addition, in the closer view shown in Fig. 5b, a straight line is traced to separate two regions. In the lower region, the trajectory is smoother than in the upper one. This leads to an antisymmetric motion of the slider on the turntable. Due to the two types of stick-slip oscillations explained before. Fig. 5b is also a justification for the selection of this particular case, due to the clear presence of stick-slip.

B. Particular case M_3 and Ω_1

Studying the phase plots of radius and angle (Fig. 6) the antisymmetry is again present.

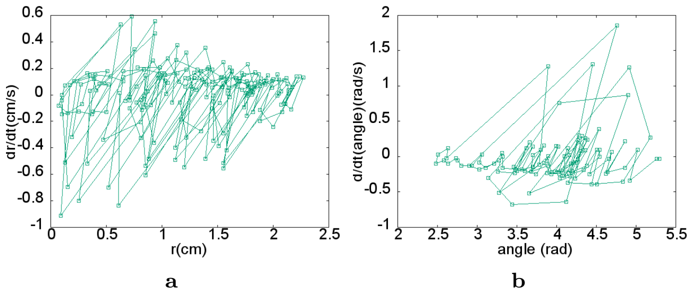

FIG. 6: Phase plots of radius and angle. (a) $\dot{r}(r)$ with spring. (b) $\dot{\theta}(\theta)$ with spring.

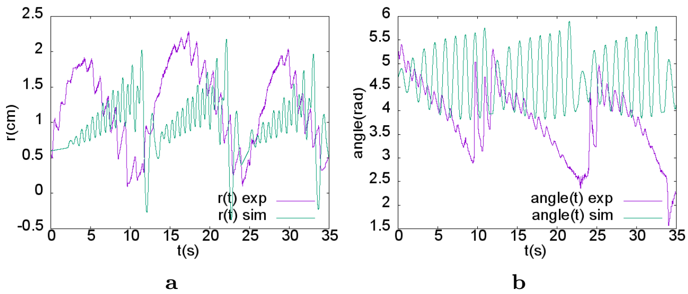

FIG. 7: Comparison of the Coulomb model simulation and the experimental results for the particular case. (a) $r(t)$ with spring. (b) $\theta(t)$ with spring.

In Fig. 6a the radius tends to decrease more than increase and in Fig. 6b the angle tends to increase more than decrease. Some large peaks can be observed in both Fig. 6a and Fig. 6b that correspond to large amplitude stick-slip. They can be identified in Figs. 3b and 3d. The smaller peaks correspond to small amplitude stick-slip motions which can also be identified in Figs. 3b and 3d.

Using the stick-slip conditions in Eq. (2) and the equations of motion of the slider (Eq. (4)), it is possible to compare the experimental results with the numerically-simulated dynamic behaviour of the Coulomb model in 2D (Fig. 7). Remarkably the Coulomb model predicts the periods of the stick-slip with no fitting parameters, but it is not able to reproduce well the system dynamics.

IV. CONCLUSIONS

In this work a new experimental setup has been designed in order to study two-dimensional friction dynamics and to detect the nonlinear behavior of friction. We have compared qualitatively a steady sliding case and a case that presents non-linear behavior. In particular, two types of stick-slip motion have been observed in the results, one due to the harmonic behavior of the mass-spring system and the other caused by the change of the relative velocity between surfaces. In the framework of the Coulomb model, the equations of motion have been solved numerically and compared with the results, but this model just predicts the periods of the stick-slip.

To improve this work, it would be interesting to compare the experimental results with other friction models with dependence velocity or time dependence in the friction coefficient.

Acknowledgements

I would like to thank my advisors Jordi Ortín and Ramon Planet for their dedication; Xavier Santana and Jordi Pastor for helping me with the set up of the turntable and the fabrication of the slider; and my family and friends for the support received during my studies.

[1] Andersson, S., Söderberg, A., Björklund, S.. “Friction models for sliding dry, boundary and mixed lubricated contacts”. Tribology International, **40**, 580–587 (2007)
[2] Matsukawa H., Saito T.. ”Friction, Stick-Slip Motion and Earthquake”. Lecture Notes in Physics, **705**, 169-189 (2006)
[3] Bowden F.P., Tabor D.. “Friction, lubrication and wear: a survey of work during the last decade”. British Journal of Applied Physics, **17(12)**, 1521-1544 (1966)
[4] H. Butt, K. Graf and M. Kappl, *Physics and Chemistry of Interfaces: Chapter 11* (Editors: H. Butt, K. Graf and M. Kappl, John Wiley and Sons, New York 2004), 223-245
[5] Ananthakrishna, G., De, R.. “Dynamics of Stick-Slip: Some Universal and Not So Universal Features”. Lecture Notes in Physics, **705**, 423-457 (2006)
[6] Martins, J.A.C., Oden, J.T., Simões, F.M.F.. “A study of static and kinetic friction”. International Journal of Engineering Science, **28(1)**, 29-92 (1990)
[7] Heslot, F., Baumberger, T., Perrin, B., Caroli, B., Caroli, C.. “Creep, stick-slip, and dry-friction dynamics: Experiments and a heuristic model”. Physical Review E, **49(6)**, 4973-4988 (1994)
[8] E. Rabinowicz, *Friction and Wear of Materials*, (Wiley, New York 1995)
[9] Tapia, F., Le Tourneau, D., Géminard, J.-C.. “Anisotropic friction: assessment of force components and resulting trajectories”. EPJ Techniques and Instrumentation, **3(1)**, (2016)
[10] Agha, A., Gupta, S., Joseph, T.. “Particle sliding on a turntable in presence of friction”. Am. J. Phys., **83(2)**, (2015)